Environmental Science and Pollution Research (2019) 26:24430–24444
https://doi.org/10.1007/s11356-019-05676-z

RESEARCH ARTICLE

Differential growth, nutrition, physiology, and gene expression in *Melissa officinalis* mediated by zinc oxide and elemental selenium nanoparticles

Alameh Babajani[1] · Alireza Iranbakhsh[1] · Zahra Oraghi Ardebili[2] · Bahman Eslami[3]

Received: 25 January 2019 / Accepted: 4 June 2019 / Published online: 22 June 2019

Abstract

Regarding the rapid progress in the production and consumption of nanobased products, this research considered the behavior of *Melissa officinalis* toward zinc oxide nanoparticles (nZnO), nanoelemental selenium (nSe), and bulk counterparts. Seedlings were irrigated with nutrient solution containing different doses of nZnO (0, 100, and 300 mg l^{-1}) and/or nSe (0, 10, and 50 mg l^{-1}). The supplements made changes in growth and morphological indexes in both shoot and roots. The mixed treatments of nSe10 and nZnO led to a drastic increase in biomass, activation of lateral buds, and stimulations in the development of lateral roots. However, the nSe50 reduced plants' growth (45.5%) and caused severe toxicity which was basically lower than the bulk. Furthermore, the nSe and nZnO improved K, Fe, and Zn concentrations in leaves and roots, except for seedlings exposed to nSe50 or BSe50. Moreover, the nSe and nZnO supplementations in a dose-dependent manner caused changes in leaf non-protein thiols (mean = 77%), leaf ascorbate content (mean = 65%), and soluble phenols in roots (mean = 28%) and leaves (mean = 61%). In addition, exposure to nZnO and/or nSe drastically induced the expression of rosmarinic acid synthase (RAS) and Hydroxy phenyl pyruvate reductase (HPPR) genes. Besides, the nSe, nZnO, or bulk counterparts influenced the activities of nitrate reductase in leaves and peroxidase in roots, depending on dose factor and compound form. The comparative physiological and molecular evidence on phytotoxicity and potential advantages of nSe, nZnO, and their bulk counterparts were served as a theoretical basis to be exploited in food, agricultural, and pharmaceutical industries.

Keywords Metal oxide · Nanofertilizer · Nanoparticle · Selenium · Toxicity · Zinc oxide

Introduction

In nature, selenium (Se, metalloid mineral) is detected in various ionic species, including organic, selenate (VI), selenite (IV), elemental Se (0), and selenide (-II) (Hu et al. 2018). It is worth noting that Se is classified as an essential mineral for a multitude of living forms such as humans, while its advantages in plant life cycle and probable need for it are still under debate (Ardebili et al. 2015; Nazerieh et al. 2018; Safari et al. 2018; Babajani et al. 2019). Considering dietary requirements of humans (55 μg day^{-1}, according to the Food and Nutrition Board of the Institute of Medicine (USA)), fertilization of cultivating plants with Se has been emphasized in order to improve the Se concentrations (especially in an organic form) in various plant-derived foods (Tang et al. 2017; Babajani et al. 2019), although Se at high doses (varied ranges depending on plant species, developmental stage, Se sources, and utilization method) might be a toxic limiting factor (Safari et al. 2018; Babajani et al. 2019). The potential advantages of Se in plant growth, physiology, and protection have been supported by several lines of previous studies (Ardebili et al. 2015; Djanaguiraman et al. 2018; Safari et al. 2018). Moreover, in tomato, Se at low levels postponed senescence, reduced ethylene synthesis, declined respiration rate, delayed fruit ripening, and modified postharvest life through controlling the expression of genes involved in ethylene biosynthesis,

Responsible editor: Gangrong Shi

✉ Alireza Iranbakhsh
iranbakhsh@iau.ac.ir

[1] Department of Biology, Science and Research Branch, Islamic Azad University, Tehran, Iran

[2] Department of Biology, Garmsar Branch, Islamic Azad University, Garmsar, Iran

[3] Department of Biology, Ghaemshahr Branch, Islamic Azad University, Ghaemshahr, Iran

and boosting the antioxidant defense system (Zhu et al. 2017). Hence, Se application has been introduced as a promising method for delaying senescence and fruit ripening process and improving the shelf life (Zhu et al. 2017). In addition, Tang et al. (2017) reported that soil supplementation with Se instead of foliar application prevented mercury (Hg: an important heavy metal contaminant) accumulation in rice, indicating antagonistic interactions between Hg and Se. The nanoparticle of elemental red Se (nSe) has been functionalized in the pharmaceutical industries, due to its bioactivity, efficient antioxidant, anticancer, and antimicrobial properties (Hu et al. 2018). The exposure to nSe improved plant protection against heat stress in sorghum (Djanaguiraman et al. 2018). In addition, expression patterns of heat shock factor A4A (HSFA4A) were altered following nSe exposure in *Triticum aestivum* (Safari et al. 2018). Nazerieh et al. (2018) showed both benefits and toxicity of nSe in peppermint. However, there is limited data concerning plant reactions to nSe exposure, especially supplementation of the nutrient solution instead of foliar application that needs to be explored further.

Zinc (Zn) is an essential mineral nutrient that plays critical roles as a vital limiting factor toward plant growth, development, productivity, and protection. Zn deficiency in plants provokes biomass and yield reduction, necrotic symptoms, and chlorosis of leaves. Zn influx may primarily mediate through the carriers belonging to the ZIP (ZRT, IRT-like) protein family and the voltage-gated cation channel (Bouain et al. 2014). Zn plays crucial roles in six enzymatic classes (lyases, oxidoreductases, hydrolases, transferases, ligases, and isomerases) and has many functions in regulatory proteins (Bouain et al. 2014). Considering the vital roles of Zn on human health, crop bio-fortifying with essential nutrients and improving the productivity of crops have received much attention (Bouain et al. 2014). Therefore, modern agricultural activities extensively require development of novel formulations for nutrient solutions, fertilizers, and pesticides (Bouain et al. 2014).

The nanoparticles of metal oxides have specific physiochemical traits (surface, electrical, thermal, and optical) different from their bulk counterparts (Rastogi et al. 2017). Among different metal oxide nanoparticles, the most commercially utilized ones in different industries are zinc oxide (nZnO), silver, titanium dioxide, cerium dioxide, and copper oxide (Rastogi et al. 2017). Application of nZnO at suitable concentrations (based on the plant species, developmental stage, and treatment method) modified the growth, physiology, and protection of different plant species, such as *Leucaena leucocephala* (Venkatachalam et al. 2017a), *Zea mays* (Subbaiah et al. 2016), and *Pisum sativum* (Mukherjee et al. 2016), while it caused phytotoxicity in *Oryza sativa* (Salah et al. 2015), *Arabidopsis* (Wang et al. 2016), and *Capsicum annuum* (Iranbakhsh et al. 2018) at high doses. There is limited and contradictory evidence for plant reactions following nZnO exposure; hence, further precise studies are required to elucidate its possible effectiveness or phytotoxicity.

Demand for nanobased products in various industries, especially food, medicine, and agriculture, is extensively boosting (Moghanloo et al. 2019; Seddighinia et al. 2019). Due to the high consumption of nanoparticles, their introduction into the food chain, particularly through plant-derived seed, drug, or foods, is inevitable. Therefore, cogent studies are needed to clarify various aspects of eco-toxicological impacts of nanoparticles. Recent findings indicate that different manufactured nanoparticles exhibit potential advantages in agriculture and postharvest life. As a result, these compounds may be exploited in modern food and agricultural-related industries (Rastogi et al. 2017; Asgari-Targhi et al. 2018; Seddighinia et al. 2019). Different strategies have been taken to develop more effective novel alternative fertilizers and pesticides based on nanomaterials (Moghaddasi et al. 2017; Asgari-Targhi et al. 2018; De Francisco and García-Estepa 2018; Seddighinia et al. 2019). Interaction of nanoparticles and biomolecules depends on several key factors, including shape, size, surface, purity, stability, and manufacturing method (Rastogi et al. 2017; Asgari-Targhi et al. 2018). Therefore, more studies are required to illustrate the role of nanoparticles in plants' life and clarify the mechanisms contributing to these kinds of plant interactions. This might provide a scientific basis for their possible application in technology as well as industry.

Melissa officinalis (lemon balm, a perennial herb, a member of Lamiaceae) has an outstanding phytochemistry (the phenylpropanoid derivatives and the essential oils), in which terpenoids, rosmarinic acid, caffeic acid, protocatechuic acid, and flavonoids are the main secondary metabolites. *M. officinalis* is commercially applied in traditional and modern pharmaceutical industries. There are several drugs made from lemon balm for the treatment of different human diseases, including cancer, Alzheimer, migraine, and rheumatism (Moradkhani et al. 2010). The prominent phenylpropanoid derivative in lemon balm is rosmarinic acid exhibiting a multitude of interesting biological functions (antioxidant, anti-inflammatory, antibacterial, and antiviral). Consequently, diverse attempts have been made to trigger production of rosmarinic acid (Tonelli et al. 2015). The biosynthesis pathway of rosmarinic acid as an important secondary metabolite and contributing enzymes is depicted in Fig. 1. Hydroxy phenyl pyruvate reductase (HPPR) and rosmarinic acid synthase (RAS) are two key enzymes involved in the tyrosine-derived biosynthesis of rosmarinic acid. The existence of a close correlation between the expression of the RAS gene and the RAS activity in suspension cultures of lemon balm has been reported (Weitzel and Petersen 2011). It has been stated that the nanoparticles may modify intracellular redox status through which the transcription profiles might be reprogrammed

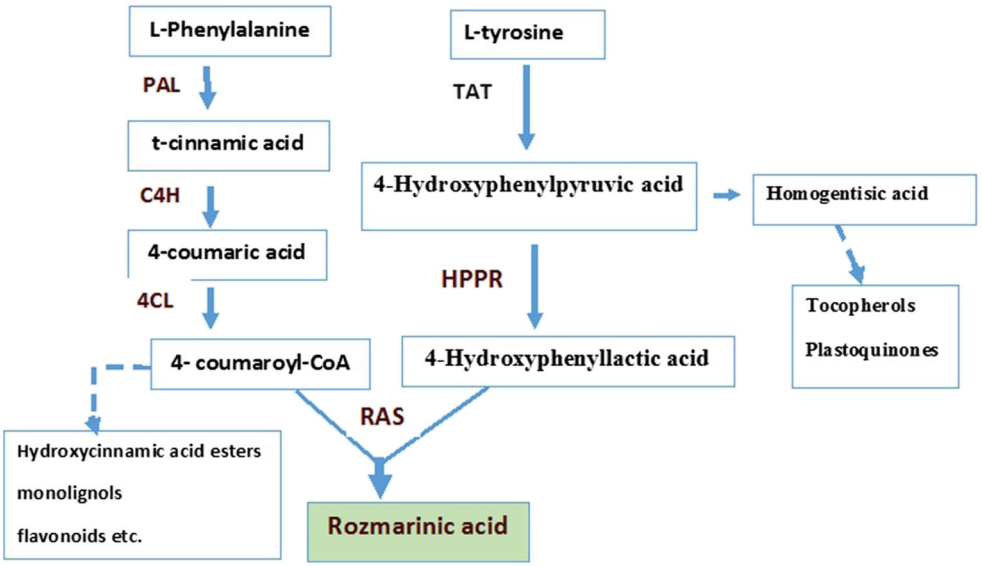

Fig. 1 The identified biosynthesis route for rosmarinic acid with several side processes in *M. officinalis* is represented by Weitzel and Petersen (2011). PAL, phenylalanine ammonia lyase; C4H, cinnamic acid 4-hydroxylase; 4CL, 4-Coumarate: CoA-ligase; TAT, tyrosine amino transferase; HPPR, Hydroxy phenyl pyruvate reductase; RAS, Rosmarinic acid synthase

(Safari et al. 2018). We, therefore, aimed at exploring the possible effects of nSe and nZnO on the expression patterns of HPPR and RAS as checkpoints.

The major aims of this experiment were to explore the possible effects of nSe, nZnO, and their bulk counterparts on (I) growth, morphology, and toxicity; (II) nutrition; (III) antioxidants; (IV) secondary metabolism markers; and (V) transcription of HPPR and RAS genes in *M. officinalis*.

Material and methods

Material preparation and characteristics of nanomaterials

The nZnO compound having size of 10–30 nm was purchased from the reliable company (US research nano materials, Inc; 3302 Twig Leaf Lane Houston, TX 77084, USA). The nSe of 10–45 nm (CAS# 7446-08-4; APS, 10–45 nm; density, 3.89 g cm^{-3}; high purity, 99.95%; morphology, spherical) was bought from the NanoSany Corporation, Iranian Nanomaterials Pioneers Company, Mashhad City, Khorasan Province, Iran. It should be noticed that this nanoproduct was provided in form of red solution of 1000 mg l^{-1} containing 0.1% polyvinylpyrrolidone (PVP) as stabilizer. The solutions of nanocompounds were ultra-sonicated using an ultrasonicator (40 kHz and 100 W powers) for 30 min to fully disperse the nanoparticles. In addition, the other physico-chemical traits of the nanocompounds were estimated based on different methods, including UV-Vis spectrophotometry, Transmission Electron Microscopy (TEM), and Field Emission Scanning Electron Microscopy (FESEM; ZEISS SIGMA VP, Germany). Furthermore, zeta potential index for each nanomaterial was quantified by Zetasizer (Malvern, UK).

Growth condition and treatments

Seeds of *M. officinalis* were grown in pots (l Kg pots; four pots for each treatment group) containing vermiculite and perlite (1:1 *v*/*v*) under the same natural conditions in Babol (Mazandaran Province, Iran; temperature, 24/16 °C day/night; relative humidity of 70%; light intensity, 65 μmol m^{-2} s^{-1}). The 40-day-old seedlings were grouped in 13 treatment groups and treated with different doses of nSe (0, 10, and 50 mg l^{-1}), nZnO (0, 100, and 300 mg l^{-1}), and their bulk counterparts. Details and descriptions of each treatment group are presented in Table 1. At first, we aimed at determining the filed capacity of the applied soilless medium. It was estimated to be 50 ml per pot (1 Kg). So, in each irrigation time, we used 70 ml nutrient solution per pot to make sure about washing the pervious nutrient solution. The seedlings were irrigated with nutrient solution containing different doses of nSe and/or nZnO (70 ml per pot per each irrigation time), twice a week. For the rest of the days, seedlings were irrigated with distilled water. We carried out this experiment in the soilless condition in order to keep the concentrations almost constant, as Hoagland solution would be washed away by watering and addition of new Hoagland solution. In case of using soil medium, the concentrations would not remain the same and result in over accumulations of elements in soil medium.

Table 1 Descriptions of 13 different treatment groups are presented. In soilless condition, seedlings were irrigated with Hoagland nutrient solution containing different doses of nanoproducts twice a week and the rest of the days with water (for 6 weeks)

Group name	Treatment description	Equal concentrations of nanoproducts per pot (mg Kg^{-1})
C	Control, irrigated with Hoagland nutrient solution	0
BSe10	Irrigated with Hoagland solution supplemented with bulk Se of 10 mg l^{-1}(SeO_2, Se (IV) oxide	0.5
nSe10	Irrigated with Hoagland solution containing nSe of 10 mg l^{-1}	0.5
BSe50	Irrigated with Hoagland solution containing bulk Se of 50 mg l^{-1}	2.5
nSe50	Irrigated with Hoagland solution supplemented with nSe of 50 mg l^{-1}	2.5
BZn100	Irrigated with Hoagland solution supplemented with bulk ZnO of 100 mg l^{-1}	5
nZn100	Irrigated with Hoagland solution containing nZnO of 100 mg l^{-1}	5
BZn300	Irrigated with Hoagland solution supplemented with bulk ZnO of 300 mg l^{-1}	15
nZn300	Irrigated with Hoagland solution containing ZnO of 300 mg l^{-1}	15
nSe10+nZnO100	Irrigated with Hoagland solution supplemented with nSe of 10 mg l^{-1} and nZnO of 100 mg l^{-1}	0.5 + 5
nSe10+nZnO300	Irrigated with Hoagland solution containing nSe of 10 mg l^{-1} and nZnO of 300 mg l^{-1}	0.5 + 15
nSe50+nZnO100	Irrigated with Hoagland solution supplemented with nSe of 50 mg l^{-1} and nZnO of 100 mg l^{-1}	2.5 + 5
nSe50+nZnO300	Irrigated with Hoagland solution containing nSe of 50 mg l^{-1} and nZnO of 300 mg l^{-1}	2.5 + 15

Ninety-day-old treated seedlings (2 weeks after the last treatments) were harvested for further physiological and molecular analysis.

Characterization of K, Fe, Zn, and Se contents

Ash solution was prepared based on dry ash procedure. Briefly, 0.3 g of the oven-dried leaf samples were digested by thermal decomposition (550 °C for 6 h) using a muffle furnace. Then, HCl (1 N) as a solvent was applied to dissolve the prepared dry ash. The solutions were subjected for assessing different elements. Concentration of K in each sample was quantified by flame photometer (Sherwood Model 410 Flame photometer). Quantitative determinations of Fe and Zn were carried out using Atomic Absorption Spectroscopy (AAS; Varian, Spectr AA.200). Se contents were measured by Graphite Furnace Atomic Absorption (Thermo-Electron solaar M5 Atomic Absorption, USA).

Quantification of non-protein thiols

Non-protein thiols were spectrophotometrically quantified according to the method represented by Del Longo et al. (1993). Briefly, the leaf samples were grounded in sulphosalicylic acid solution of 5% (*w*/*v*). The assay reaction contained 0.5 ml buffer of 0.1 M phosphate buffer (pH 7), 0.5 mM EDTA, 0.1 ml of extract, and 0.5 ml of 1 mM DTNB. The mixture was incubated for 10 min and then, the absorbance was monitored at 412 nm.

Determination of ascorbate contents

Measurement of ascorbate concentration was spectrophotometrically conducted based on the reduction phenomenon of Mo (VI) to Mo (V) at an acidic pH condition. Briefly, the reaction mixture contained leaf extract, 4 mM $(NH4)_6Mo_7O_{24}.4H2O$, 28 mM NaH_2PO_4, and 0.6 M H_2SO_4. After incubation at 95 °C for 90 min, the samples were cooled and the absorbance was measured at 695 nm. The ascorbate contents were calculated using molar absorption coefficient of 3.4×10^3 M^{-1} cm^{-1}(Geneva et al. 2010; Ardebili et al. 2015).

Determination of phenolic compound

The total soluble phenols were extracted from the root and leaf organs using ethanolic solvent of 80% (*v*/*v*), quantified by the pivotal protocol of Folin-Ciocalteu reagent, and finally calculated using the standard curve of tannic acid as a standard compound (Asgari-Targhi et al. 2018).

Gene expression analysis

Leaves were stored in − 80 °C prior to RNA extraction and analysis of expression of selected genes. RNA from the grounded leaf samples in liquid nitrogen was extracted by Trizol (GeneAll Biotechonolgy Co, South Korea). Next, DNA in the extracts was eliminated using Dnase I. Then, absorbance ratio (260/280 nm) was recorded to evaluate the RNA purity with Nanodrop (Thermo Scientific™ NanoDrop Model 2000c). After that, the complementary DNA (cDNA)

was synthesized (PEQLAB, 96Grad). The forward and reverse primer sequences for Rosmarinic acid synthase (RAS; FR670523), Hydroxy phenylpyruvate reductase (HPPR; HM587131), and Tubulin (MF579140) were represented in Table 2. Real-time quantitative PCR (Applied BiosystemsStepOne™ Real-Time PCR) was utilized to quantify the expression levels of the target genes. Tubulin was selected to be a control gene (the PCR data indicated good stability in reference gene). Finally, the expression level was calculated as fold differences. It should be noted that the gene expressions were not conducted for the treatments caused toxicity.

Activities of nitrate reductase and peroxidase

The 0.1 M phosphate buffer (pH of 7.3) was applied to extract enzyme from the well-powdered fresh samples in liquid nitrogen (Iranbakhsh et al. 2018). Immediately, the homogenates were centrifuged at 4 °C and the supernatants stored as an enzyme extract at − 80 °C. To quantify the nitrate reductase activity, the reaction mixture (2.5 ml 100 mM phosphate buffer (pH 7.4), 600 μl potassium nitrate (150 mM), and 200 μl enzyme extract) was kept at 30 °C and dark condition for 1 h. Then, 50 μl Griess reagent I (sulfanilic 0.5% in half-strong acetic acid) and 100 μl Griessreagent II (α-naphthylamine 0.2% in half-strong acetic acid) were added to the reaction mixture. Finally, the absorbance amounts in 540 nm were recorded. The nitrate reductase activity was expressed in μmol NO_2^- g^{-1} fw h^{-1}. In addition, the procedure previously explained by Hemeda and Klein (1990) with slight modification was picked out to monitor peroxidase activity. Briefly, the enzyme extract was added to the reaction medium (phosphate buffer (0.05 M; pH 6.5), H_20_2, and Guaiacol). Then, absorbance variations at 470 nm per minute were quantified, and finally, the peroxidase activity was expressed in Unit E g^{-1} fw.

Statistical analysis

All data (three independent replications for each treatment group) were subjected to analysis of variance (ANOVA) using SPSS software. The mean values of each treatment group were submitted to variance analysis by the Duncan test at a level of 5% of probability.

Results

Physicochemical characteristics of the nanoparticles

The diverse physicochemical traits of both nanoparticles were depicted in Fig. 2a–f. To prove the nature and stability of nSe, the scan spectrum curves of two different concentrations were recorded at three times with 1-h intervals (Fig. 2a). Interestingly, the sharp peak was observed around 190 nm (UV region), confirming the presence of the nanoparticles (Fig. 2a). Furthermore, there was no differential spectrum curve relative to the observed times, manifesting the stability of the nSe solution (Fig. 2a). In addition, it should be noted that the red nSe product was containing 0.1% polyvinylpyrrolidone (PVP) as stabilizer; there was no sign of sedimentation in the nSe solutions. Moreover, there was no change in the transparency of the nSe solution. Also, zeta potential value was quantified to evaluate the surface charge and nanoparticle stability by estimating the balance between the attractive and repulsive forces. The zeta potential value for nSe was − 6.32 mV (the negative surface charge) which is confirming colloidal stability owing to electrophoretic excretion (Fig. 2b). The approximate mean size of the nSe was estimated to be 22 nm (Fig. 2c). Moreover, the sharp peaks in the scan spectrum curve of nZnO at the UV range exhibited the existence of nanocompound (Fig. 2d). Interestingly, the zeta potential for the utilized nZnO was − 26.6 mV, showing high effective negative surface charges and electrostatic repulsion (Fig. 2e). Therefore, the nanoparticle stability was supported by the magnitude of zeta potential. It is crystal clear that size, zeta potential, and UV-Vis spectrum are considered as main physicochemical traits of nanomaterials, thereby controlling their interactions with plant cells (Asgari-Targhi et al. 2018). As it was depicted in Fig. 2f, the average size of the nZnO was measured to be 29.3 nm. Taken collectively, the utilized nanoparticles in the current research exhibited suitable physicochemical traits in terms of UV-Vis spectrum, zeta potential, and size, thereby interacting with plant cells at different physiological and molecular levels.

Morphology and growth

The nSe and/or nZnO treatments not only changed growth but also provoked the morphological differences in both shoot and roots when compared to the untreated control. The nSe of 50 mg l^{-1} reduced growth and caused severe toxicity (Fig. 3i, l, and m), while a moderate toxicity was recorded for the BSe50 treatment (Fig. 3g). Reductions in growth-related indexes, inhibitions in root development (especially lateral roots), and necrosis in plant lower leaves were the major toxicity signs associated with the nSe50 treatments. On the other hand, the nSe10+nZn100 and nSe10+nZn300 treatments led to a drastic increase in growth and activation of lateral stem buds (Fig. 3j, k). Interestingly, lengths of petiole and internodes, leaf area, and the number of produced leaves were changed by the nSe and nZnO (Fig. 3). It should be noted that the observed bending in the stems of the BSe- or nSe-supplemented seedlings clearly manifested enhancement in ethylene production and accumulation (Fig. 3).

Similarly, the morphology and development of root system were influenced by the treatments in dose- and type-

Table 2 Forward and reverse primer sequences for Rosmarinic acid synthase (RAS; FR670523), Hydroxyphenylpyruvatereductase (HPPR; HM587131), and Tubulin (MF579140)

Primer name	Sequence (5-3)	Tm	Amplicon (bp)
RAS-F	CCCCGACCTCAACCTTATCCC	61.9	117
RAS-R	TTTGCCACGCCTAAGCCCAC	62	
HPPR-F	GGATTTGGCGATCGGGTTGAT	61	185
HPPR-R	CAAATGCCTCTGCTCGCTCAG	61	
Tubulin-F	ATTTGATTCCATTCCCACGTCT	60	117
Tubulin-R	CCCACATTTGTTGCGTTAGC TC	59	

dependent manners (Fig. 4a–m). Application of nZnO intensely altered root architecture by enhancing the development of lateral roots which was a specific reaction to nanoform contrary to the bulk (Fig. 4), while the BSe or nSe of 10 mg l^{-1} elevated the root lengths and restricted the emergence of lateral roots. Moreover, the nSe50 supplementation provoked extreme reduction in root system (Fig. 4).

The BSe50 treatment led to a moderate significant ($P \leq 0.05$) decrease in total leaf fresh mass by 29% which was much less than the rate recorded for the nSe50-treated plants (approximately 45.5% , Fig. 4). The combined treatments of nSe10 and nZnO caused a drastic increase (around 64%) in the total leaf fresh weight, while the moderate significant enhancements were recorded for the individual treatments of nSe10, BZnO, and nZnO (Fig. 5).

Nutritional status

The nSe50 applications significantly reduced the K concentrations in leaves by 27%, whereas only a slight decrease (12%) was found for the BSe50 group (Fig. 6a). Moreover, the highest amount of K concentrations in leaf organ were recorded in the nSe10+nZn100 (18.5%) and nSe10+nZn300 (35.4%) groups, over the control (Fig. 6a). The BSe50 treatment diminished the root K levels by 21%, while the BSe10 did not make a significant change (Fig. 6b). However, the nSe50 treatments significantly reduced the K levels in root (Fig. 6b). The individual and combined treatments of nZn100 were much more effective treatments to enhance the K contents in root than the nZn300 (Fig. 6b). Similarly, the nSe50 treatment exhibited severe toxicity and diminished leaf Fe content by approximately 42% when compared to the control (Fig. 6c). Interestingly, the nZn100, nZn300, nSe10+nZn100, and nSe10+nZn300 treatments led to significant elevation in Fe concentrations in leaves around 67.7%, over the control (Fig. 6c). Fe concentrations in roots of BZn100, BZn300, nZn100, nZn300, nSe10+nZn100, and nSe10+nZn300 groups were significantly higher than the control by mean of 24% (Fig. 6d). The BSe50 or nSe50 treatments adversely affected the Fe content in roots by approximately 47% (Fig. 6d). The BZn300 (74%), nZn100 (61%), nZn300 (twofold), nSe10+nZn100 (51.8%), and nSe10+nZn300 (80.9%) treatments significantly increased leaf Zn in comparison to the control (Fig. 6e). However, the individual nSe50 treatment resulted in decreased Zn content in leaf by 31.6%, relative to the control (Fig. 6e). It should be noted that Se was not detected in the C, BZn100, BZn300, nZn100, or nZn300 groups (Fig. 6f). The leaf Se content in plants individually supplemented with the nSe (10 or 50 mg l^{-1}) was higher by approximately 50% than the bulk form, exhibiting its higher potencies of uptake and/or mobilization (Fig. 6f).

Non-protein thiols, ascorbate, and total soluble phenols

The nSe10, nSe10+nZn100, and nSe10+nZn300 treatments provoked the drastic and significant ($P \leq 0.05$) increase in the leaf non-protein thiols about twofold over the control (Fig. 7a). Moreover, the ascorbate contents in leaves were dramatically augmented in the BZn300, nSe10+nZn100, and nSe10+nZn300 treatments about twofold when compared to the control (Fig. 7b). In addition, the other groups had higher ascorbate contents over than the control by mean of 50% (Fig. 7b).

Total soluble phenols in leaves were affected by the applied treatments mainly in a dose- and type-dependent manner, where the nanoforms were more efficient than the bulk (Fig. 7c). The nSe10, nZn100, nSe10+nZn300, and nSe50+nZn300 groups had the highest amount of the leaf soluble phenols by approximately twofold compared to the control (Fig. 7c). Significant and extreme increases in the root soluble phenols were caused by BSe50, nSe50, nSe50+nZn100, and nSe50+nZn300 treatments (about twofold) (Fig. 7d). Also, the individual or combined treatments of nSe10 provoked increase in root soluble phenols around 42% (Fig. 7d). BZn300, nZn100, and nZn300 treatments led to slight reductions in root soluble phenols (Fig. 7d).

Gene expression

In comparison to the untreated control, the nSe10, nZnO100, nZnO300, and nSe10+nZnO300 treatment led to a drastic

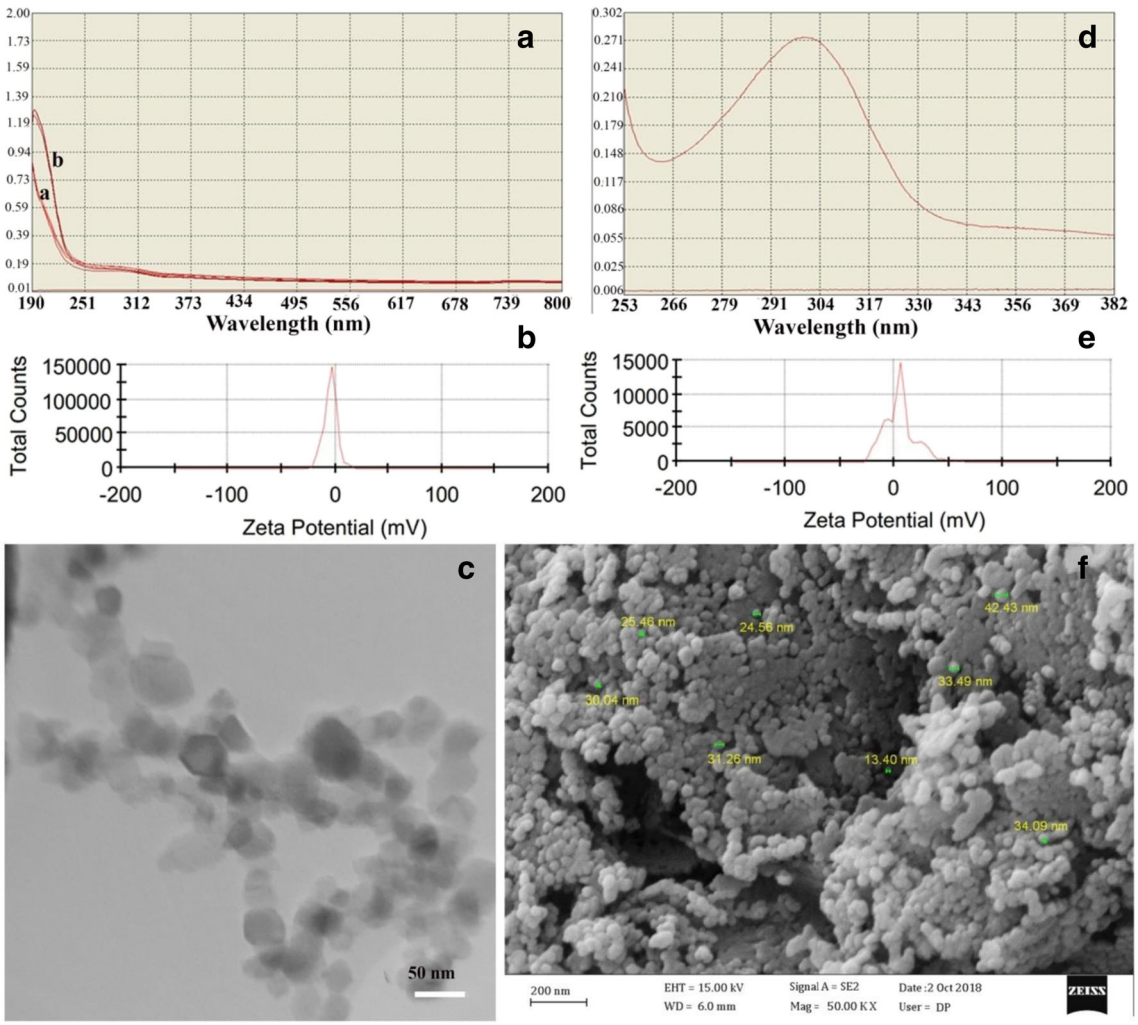

Fig. 2 The different physicochemical characteristics of the applied nSe and nZnO. **a** UV-Vis scan spectrum curves which were recorded for two concentrations of 10 mg l^{-1} (a) and 20 mg l^{-1} (b) repeated at three different times with 1-h intervals; **b** the effective zeta potential spectrum of nSe; **c** morphology and size of the nSe product; **d** UV-Vis scan spectrum curve of nZnO; **e** the effective zeta potential spectrum of nZnO. **f** Morphology and size of the nZnO

induction in the expression of HPPR, while the nSe10+ nZnO100 and BZnO300 moderately and significantly stimulated the expression of HPPR (Fig. 8a). It should be noted that the BSe10 and BZnO300 slightly enhanced the expression of this gene when compared to the control (Fig. 8a). The supplementation of nutrient solution with nSe, nZnO, and their bulk counterparts led to an intensive significant increase in the expression of RAS in the treated seedlings among which the BZnO300, nSe10, nZnO300, nZnO100, and BZnO100 groups were the highest (Fig. 8b).

Nitrate reductase and peroxidase

In contrast to the nSe50-counteracted plants, the other treatments significantly induced the activity of nitrate reductase enzyme in leaves when compared to the untreated control (Fig. 9a). The activity of nitrate reductase enzyme in the nSe50-treated plants in 3 groups was significantly ($P \leq 0.05$) lower than the control by 15% (Fig. 9a). Furthermore, the peroxidase activities in roots were found to be significantly induced in the treated seedlings. The nZn300, nSe10+ nZn100, and nSe50+nZn100 groups had the highest activities (approximately twofold over the control) (Fig. 9b).

Discussion

Growth, biomass, and nutritional status

The individual or mixed applications of nSe10 and nZnO improved plant growth indexes and biomass accumulation. Furthermore, stem bending, activations of lateral stem buds (alteration in apical dominance), modifications in leaf area, and alteration in root development were the morphological

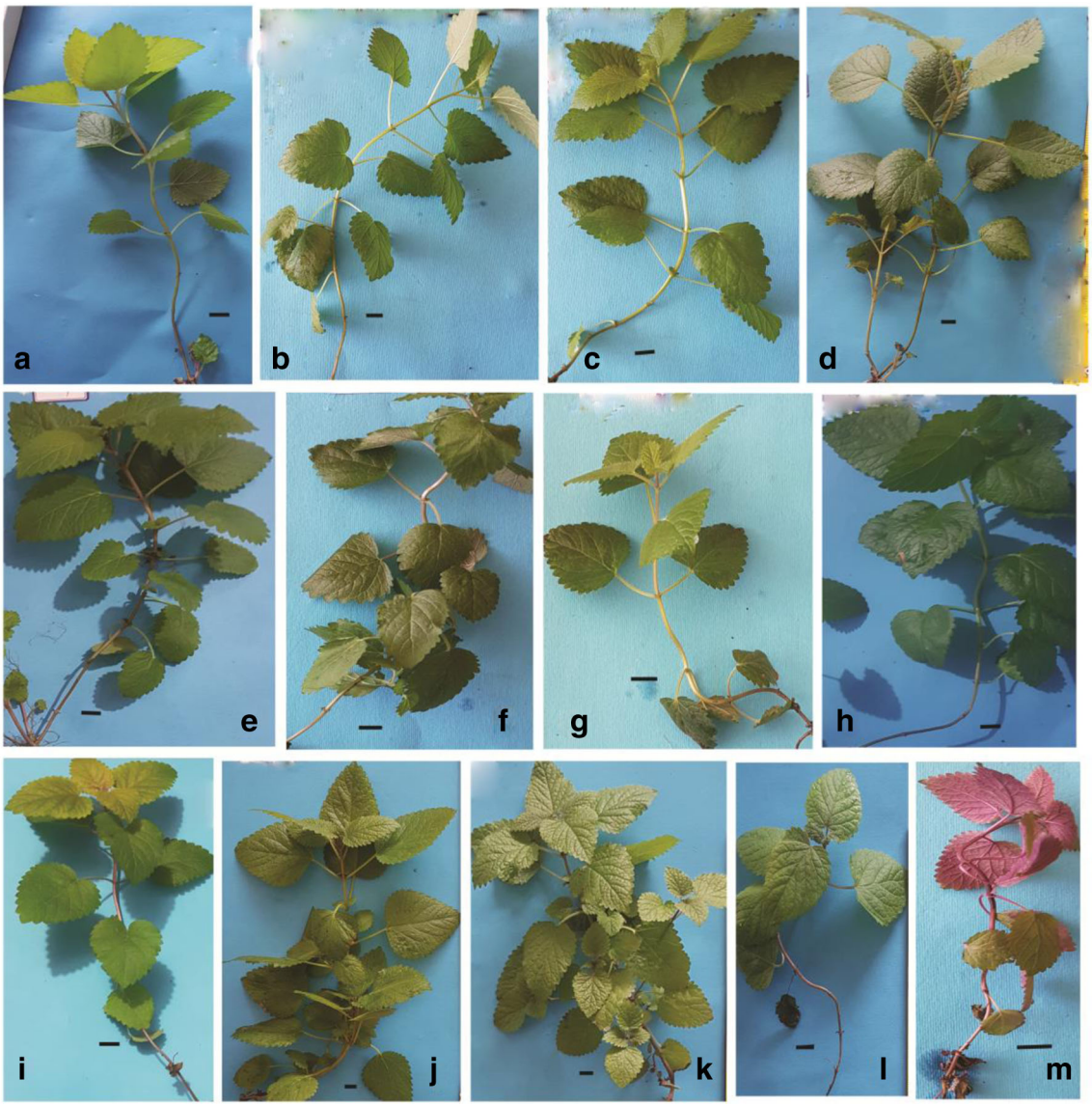

Fig. 3 The differential growth and morphology induced by supplementation of Hoagland nutrient solution with different concentrations of nSe, nZnO, and their bulk counterparts. The drawn lines in each section are 1 cm. **a** Control; **b** bulk ZnO of 100 mg l^{-1}; **c** bulk ZnO of 300 mg l^{-1}; **d** nZnO of 100 mg l^{-1}; **e** nZnO of 300 mg l^{-1}; **f** bulk Se of 10 mg l^{-1}; **g** bulk Se of 50 mg l^{-1}; **h** nSe of 10 mg l^{-1}; **i** nSe of 50 mg l^{-1} ; **j** nSe of 10 mg l^{-1} and nZnO of 100 mg l^{-1}; **k** nSe of 10 mg l^{-1} and nZnO of 300 mg l^{-1}; **l** nSe of 50 mg l^{-1} and nZnO of 100 mg l^{-1}; **m** nSe of 50 mg l^{-1} and nZnO of 300 mg l^{-1}

changes in response to nSe and/or nZnO treatments. These morphological differences underline the probable shift in hormonal balance, especially auxin and ethylene which requires being further explored. The high dose of nSe exhibited severe toxicity, whereas, the equivalent bulk counterpart made moderate phytotoxicity. In addition, the results prove the hypothesis that plant reaction to nanoproducts may be different from their reaction to their bulk counterparts. For instance, drastic change in root system (extensive root branching) was a specific response to nZnO300 treatment. This modification in root development might have been attributed to the nZnO300-associated damages in root meristem cells (possible slight toxicity) through which developments of lateral roots were stimulated. The nSe10+nZnO100 and nSe10+nZnO300 groups were the most effective treatments to modify plant morphology, growth, and physiology. Moreover, the specific morphologies (especially activation of lateral buds and root development) were observed only in these groups, reflecting different plant behavior in response to simultaneous application of nSe and nZnO compared to individual treatments. Differences in plant behavior in nanomaterials may be attributed to differential physicochemical characteristics of these compounds through which the uptake, interactions with biomolecules, signaling cascades, and biological systems of nanoparticles may be altered. According to the recent scientific experimentations, nanoparticles are more bioactive

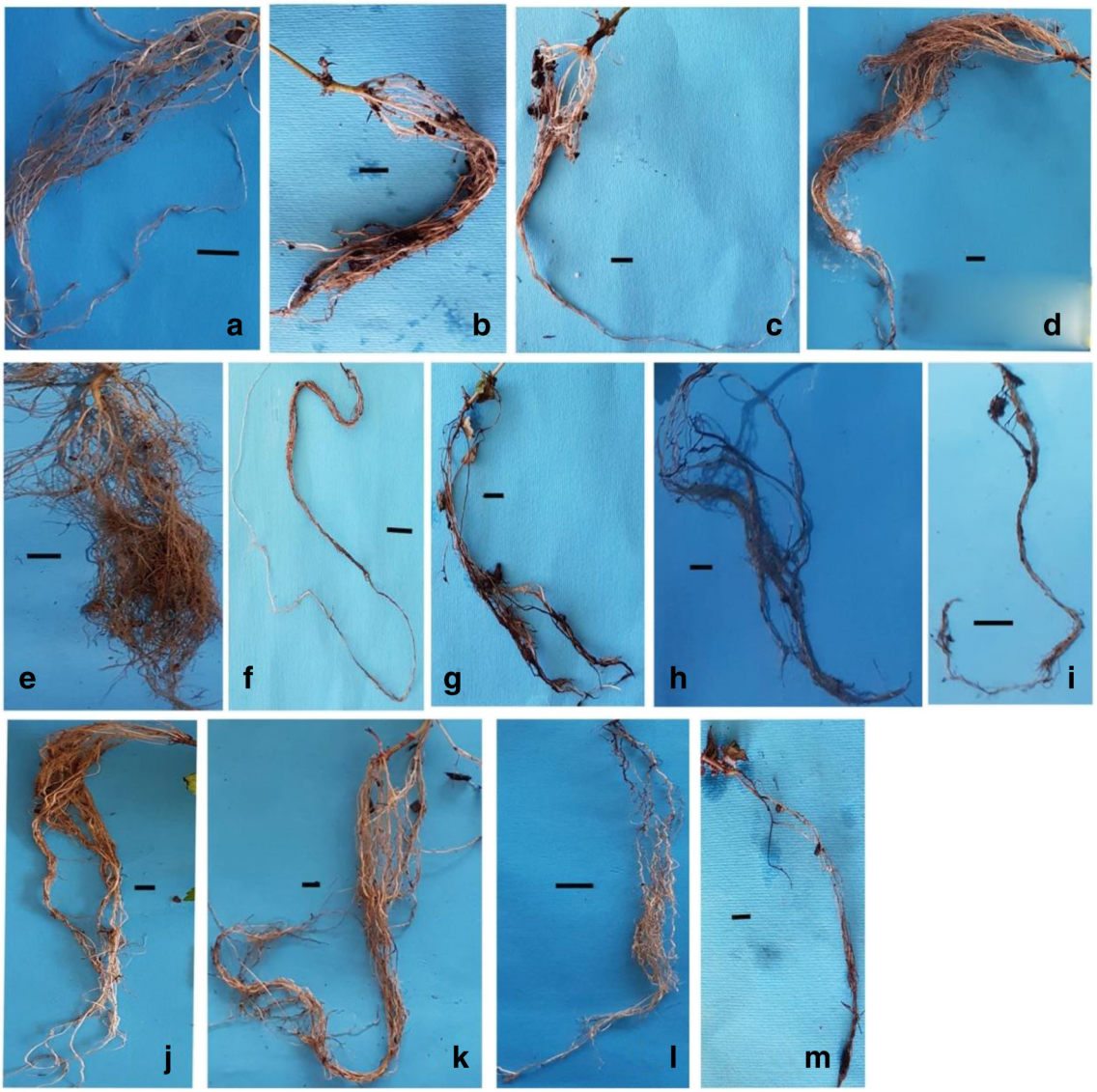

Fig. 4 The differential root growth and morphology induced by supplementation of Hoagland nutrient solution with different concentrations of nSe, nZnO, and their bulk counterparts. The drawn lines in each section are 1 cm. **a** Control; **b** bulk ZnO of 100 mg l^{-1}; **c** bulk ZnO of 300 mg l^{-1}; **d** nZnO of 100 mg l^{-1}; **e** nZnO of 300 mg l^{-1}; **f** bulk Se of 10 mg l^{-1}; **g** bulk Se of 50 mg l^{-1}; **h** nSe of 10 mg l^{-1}; **i** nSe of 50 mg l^{-1} ; **j** nSe of 10 mg l^{-1} and nZnO of 100 mg l^{-1}; **k** nSe of 10 mg l^{-1} and nZnO of 300 mg l^{-1}; **l** nSe of 50 mg l^{-1} and nZnO of 100 mg l^{-1}; **m** nSe of 50 mg l^{-1} and nZnO of 300 mg l^{-1}

agents than bulk owing to their unique physicochemical traits (Moghaddasi et al. 2017; Asgari-Targhi et al. 2018; Moghanloo et al. 2019). Differential behavior of plants to nanomaterials and bulk types has been related to surface and quantum effects. It, thereby, influences their chemical reactivity and interaction with target biomolecules, like DNA, lipids, proteins and enzymes, and other cellular components (Mehrian and De Lima, 2016). Regarding the uptake, translocation, and bioaccumulation of nZnO, it can pass through cellular membrane, interact with intracellular biomolecules (Lee et al. 2013), and be bioaccumulated (De la Rosa et al. 2013; Bradfield et al. 2017). In line with our results, nZnO (coated or uncoated nanoparticles) displayed higher bioaccessibility compared to the bulk types (Moghaddasi et al. 2017). In this research, nSe50 exhibited more toxicity in comparison to BSe50. This response may result from the higher uptake rate of nSe compared to BSe (confirmed by higher Se contents in nSe50 group than BSe50). There are limited studies in plant cells to address how nSe behave and affect plant growth, morphology, anatomy, metabolism, and transcription program. Hu et al. (2018) provided strong evidence that nSe uptake is a passive process via aquaporin which is different from the entry mechanism of other Se forms (active transport; energy-dependent transport via sulfate and phosphate transporters). The nSe application at a 50 to 100 mg kg^{-1} level increased organogenesis phenomenon and root growth in

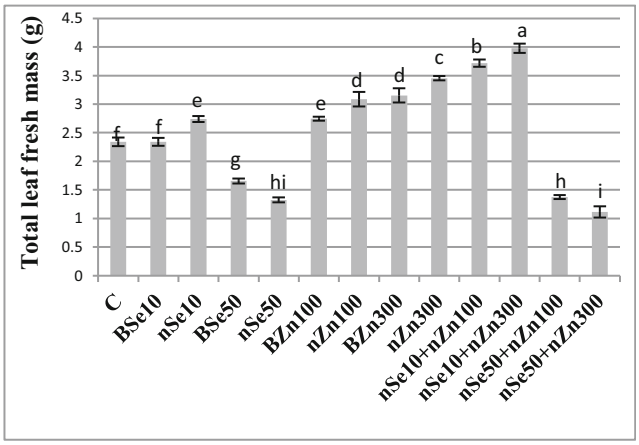

Fig. 5 The nSe, nZnO, and their bulk counterparts mediated changes in total leaf fresh mass (1 month after the treatments). Bars indicate the standard error

tobacco, in contrast to selenate. It shows its higher effectiveness and lower toxicity when compared to the bulk form (Domokos-Szabolcsy et al. 2012). Se appears to act through alterations in several plant hormones, including ethylene, jasmonic acid, and salicylic acid (Tamaoki et al. 2008; Ardebili et al. 2015; Lima et al. 2018), thereby triggering different signaling cascades, modifying metabolism, nutrition, and reprogramming expression patterns of stress-responsive genes. Likewise, nZnO in a dose-dependent way altered abscisic acid and gibberellin contents in rice (Sheteiwy et al. 2017).

There was a close correlation between the biomass and the status of essential key nutrients, including K, Fe, and Zn, each of them playing crucial structural and/or metabolic roles in plants. Improvements in nutritional status, especially due to the nZnO treatment over the bulk counterpart, could be attributed to the modification in the development of the root system. It can be a key mechanism contributing to plant nutrition. It is well known that the development of lateral roots has specific critical roles in the uptake of immobile elements, especially Fe. In line with our results, the nZnO supplementations into the culture medium enhanced the number of leaves and nodes in micropropagated *Stevia rebaudiana* (Javed et al. 2017). Also, the phyco-molecule-coated nZnO influenced meristem cells and improved biomass accumulation in cotton (Venkatachalam et al. 2017b). Moreover, expression pattern of photosynthesis-related genes was altered following the nZnO treatment (Wang et al. 2016). Inconsistent with our findings, the nZnO application led to reductions in biomass, growth, photosynthesis performance, and transpiration level (Wang et al. 2016). In addition, up-regulations in the expressions of genes involved in sulfur transportation and assimilation and stress-defensive responses have been mentioned as key mechanisms in Se-hyper-accumulators (Lima et al. 2018). The potential advantage of Se in plant growth can be attributed to Se-mediated changes in cellular nutritional status (especially S, Zn, Mn, Cu, and Fe), antioxidant system, hormonal balances, and transcription program of genes (Feng et al. 2013; Ardebili et al. 2015; Safari et al. 2018). Therefore, simultaneous application of nSe and nZnO at optimum concentrations may provoke specific signaling (partly different from the individual treatments), through which phytohormonal balances, defense system, interactions between stem cells and organs, nutritional status, and biomass are modified. This is the first pilot experiment in exploring the possible interaction of nSe and nZnO which can be applied in food, agriculture, and medicine industries. Generally, considering the necessity of Se- and Zn-enriched products for human health, nSe and nZnO compounds at optimized concentrations may be exploited as a new fertilizer in bio-fortifying plants, especially crops and medicinal species (Hu et al. 2018; Safari et al. 2018; Babajani et al. 2019). However, it is obvious that more persuasive studies are required to illustrate the elusive eco-toxicological impacts of these nanoproducts.

Non-protein thiols, ascorbate, and soluble phenols

Individual or mixed utilization of nSe, nZnO, and their bulk counterparts modified the concentration of non-protein thiols, ascorbate, and soluble phenols. The plants' responses depended on the compound type and its concentration. However, a non-linear regular relationship among concentrations, material types, bulk/nanoforms, and measured parameters was found. The nanomaterials at lower concentrations were more effective agents than the bulk forms to induce various physiological changes. Increase in non-protein thiols may play a vital role as an important protective mechanism, thereby risks associated with different stress conditions are ameliorated. It has been stated that Se exposure via rectifying sulfur uptake and metabolism enhances glutathione pool. This is a key mechanism which helps plant protection (Ardebili et al. 2015; Wu et al. 2017). Furthermore, ascorbate is known as a multifunctional signaling agent and its pool size modulates other antioxidants, especially glutathione supply (Ardebili et al. 2015). Reduced glutathione and ascorbic acid are crucial non-enzymatic antioxidants which scavenge active oxygen species and stabilize the cellular membranes. Therefore, the nSe and nZnO supplementation at low doses may improve crop protection, considering the fundamental defensive actions of ascorbate and thiols. Consistent with our results, the foliarly applied nSe resulted in increases in soluble phenols in leaves (Nazerieh et al. 2018). The phenylpropanoid pathway produces varieties of secondary metabolites as defense-related responses and is influenced by a multitude of environmental factors. The nZnO treatments in in vitro condition altered concentrations of soluble phenols and

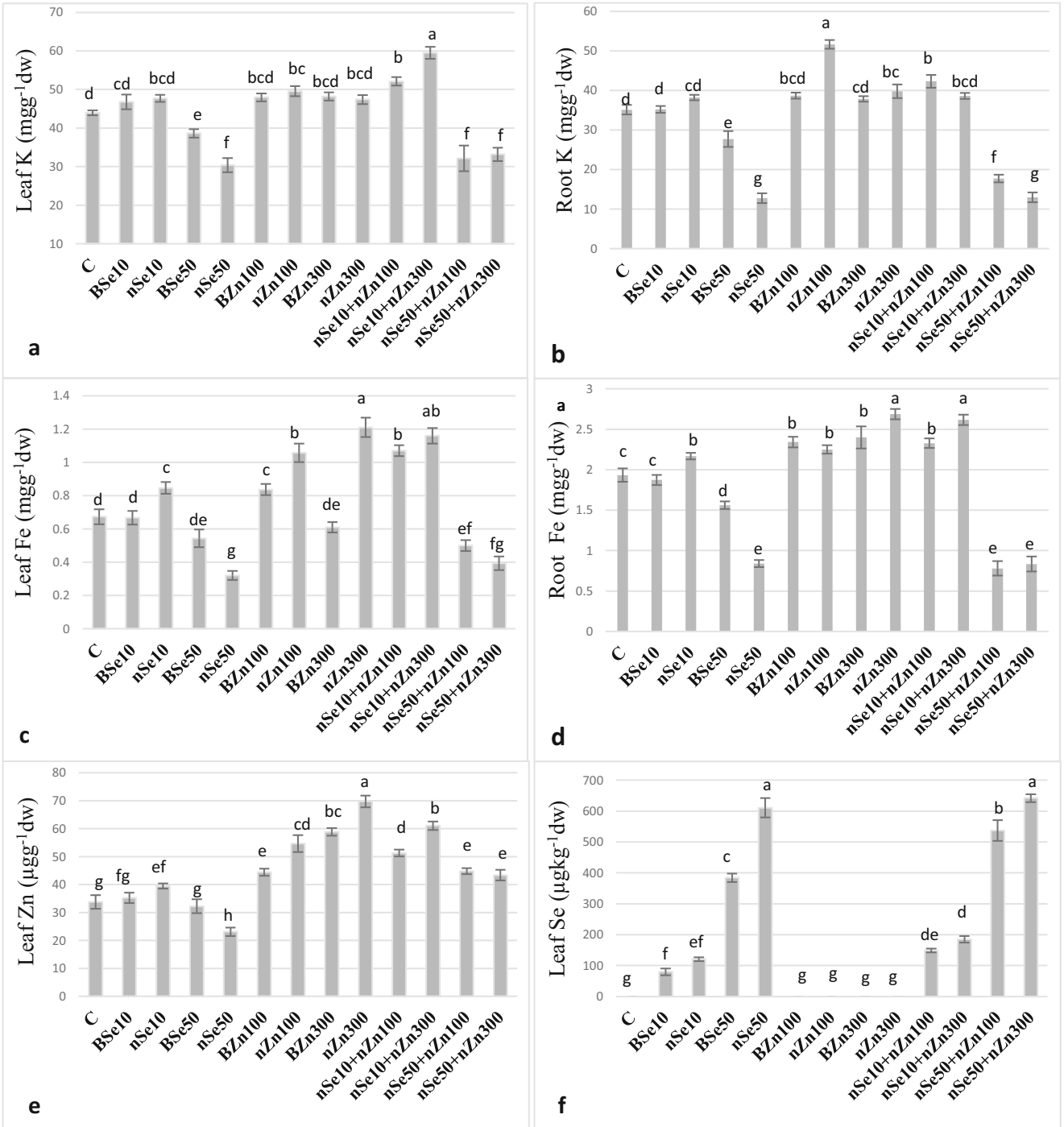

Fig. 6 **a**–**f** The differences in the nutritional status induced by the manipulation of Hoagland nutrient solution with different concentrations of nSe, nZnO, and their bulk counterparts. Bars indicate the standard error

flavonoids in *Brassica nigra* (Zafar et al. 2016) and pepper (Iranbakhsh et al. 2018). It is obvious that changes in plant secondary metabolism (especially phenylpropanoid-related exudates) may affect microbiome recruitment by which plant growth, nutrition, and protection are influenced.

Gene expression

The application of nZnO, nSe, or their bulk counterparts efficiently rectified the expression of HPPR and RAS genes. Two important enzymes were included in the biosynthesis of rozmaric acid as a very important secondary metabolite.

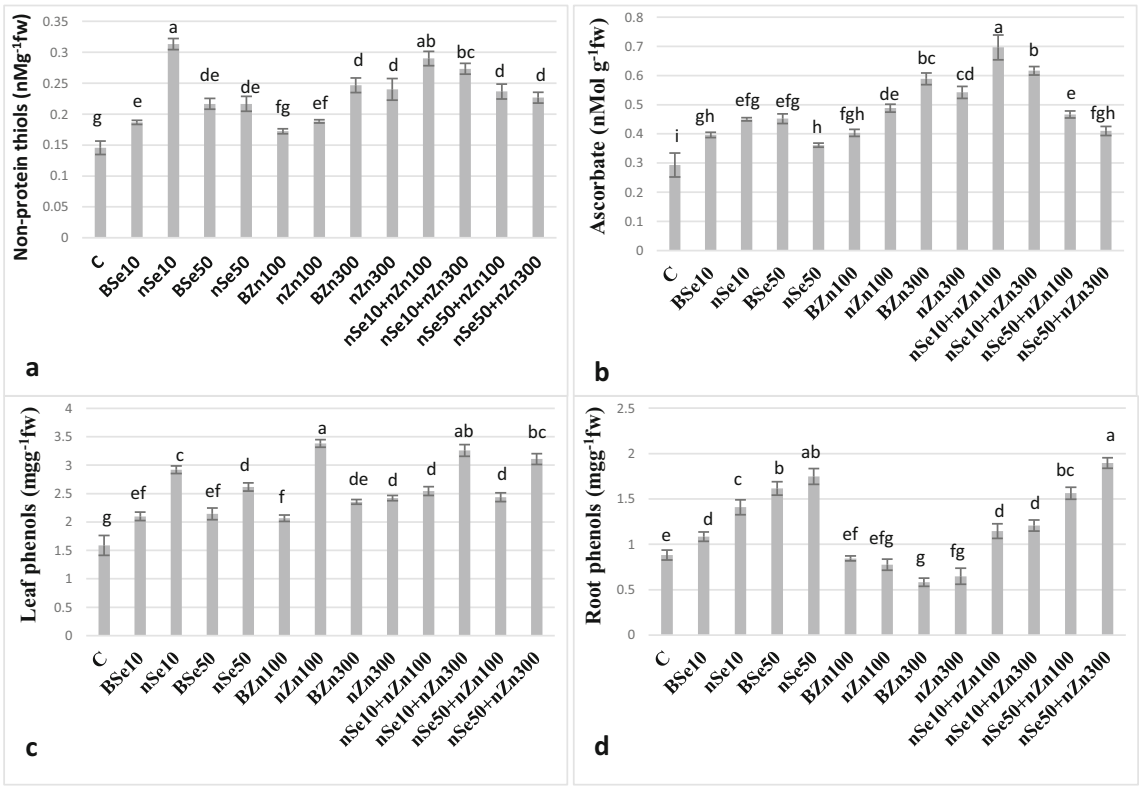

Fig. 7 **a**–**d** The induced changes in several physiological traits related to the non-enzymatic antioxidants in response to the manipulation of Hoagland nutrient solution with different concentrations of nSe, nZnO, and their bulk counterparts. Bars indicate the standard error

Secondary metabolites in plants contribute to plant adaptation and communication. However, modulations in plants' secondary metabolism in response to nanoparticles are still ambiguous. Consistently, changes in expression of heat shock factor A4A (HSFA4A, an H_2O_2 sensor and an anti-apoptosis agent) occurred following nSe exposure in wheat (Safari et al. 2018). Moreover, expression of different genes were associated with antioxidant machinery (Salah et al. 2015; Venkatachalam et al. 2017b) and photosynthesis (Wang et al. 2016) was altered in various plant species in response to nZnO exposure. However, molecular evidence on possible roles of nSe and nZnO on plant metabolism, especially secondary metabolism, is rare. Herein, valuable findings were achieved which served as theoretical foundations for the potential benefits of nZnO and nSe toward the production of secondary metabolites in *M. officinalis* (as an important pharmaceutical plant).

Nitrate reductase and peroxidase

The nSe and nZnO treatments stimulated activity of nitrate reductase, except for the high dose of nSe. At low concentrations, nanoforms of Se or ZnO were more effective than the bulk. Moreover, the synergistic effects between nSe and nZnO were not observed in the mixed treatment groups. The nSe- and nZnO-mediated changes in nutritional status, hormonal balances, and/or photosynthesis performance might have been responsible for the obtained results. In agreement with our findings, the foliarly applied nSe induced nitrate reductase in wheat (Safari et al. 2018) and peppermint (Nazerieh et al. 2018). Furthermore, exposure to Se diminished nitrate content in female *Spinacia oleracea*, in contrast to the male plant (Golubkina et al. 2017). In order to avoid photo-inhibition phenomenon, the excessive light energy should be dissipated. For this reason, nitrogen assimilation and metabolism have a close correlation with photosynthesis performance and plant acclimation during stress situation (Nazerieh et al. 2018; Safari et al. 2018). Our results are also consistent with findings of Xun et al. (2017) who reported extensive up-regulations of genes in relation to nitrogen metabolism and nutrient reservoir in the nZnO-exposed roots. Exposure to nSe and nZnO exhibited the inducing role of peroxidase activity in the root. Consistently, the foliar application of nSe provoked induction in peroxidase activity in peppermint (Nazerieh et al. 2018) and *Triticum aestivum* (Safari et al. 2018). Hereby, it is manifested that nanotypes are more efficient factors to affect peroxidase activity than their bulk counterparts. Interestingly, the nZnO treatment mitigated toxicity of heavy metals in *Leucaena leucocephala* which counteracted with Cd and Pb, via enhancing photosynthetic pigment, reducing lipid peroxidation, and inducing antioxidant enzymes (Venkatachalam et al. 2017a). Exposure to bio-engineered nZnO in *Gossypium hirsutum* induced alterations in plant morphology, improved growth,

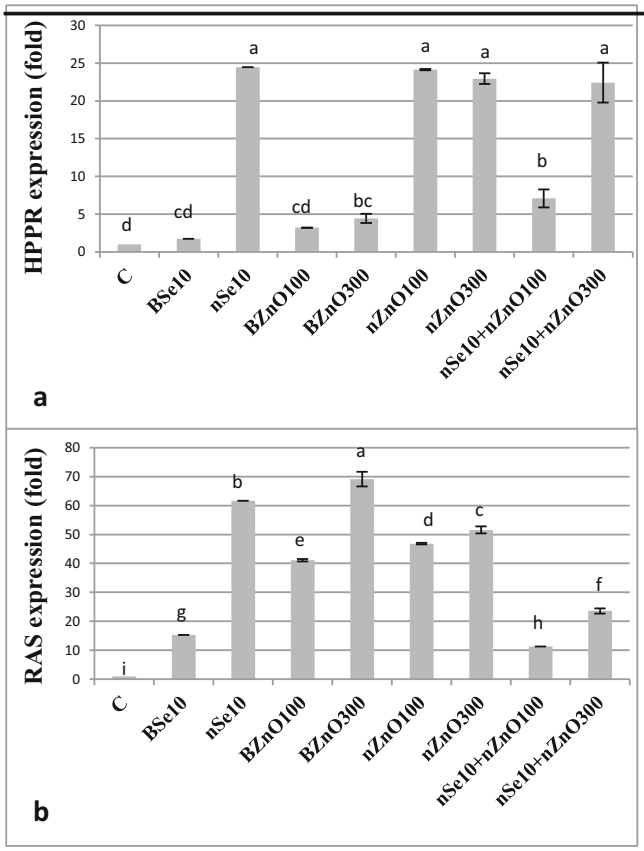

Fig. 8 **a**, **b** The changes in expression patterns of two key genes contributed to the synthesis of rosmarinic acid, including hydroxyl phenylpyruvate reductase(HPPR; HM587131) and rosmarinic acid synthase (RAS; FR670523), provoked by the manipulation of Hoagland nutrient solution with different concentrations of nSe, nZnO, and their bulk counterparts

enhanced photosynthetic pigments, modulated antioxidant system, and declined lipid peroxidation rate in cellular membranes (Venkatachalam et al. 2017b). The nZnO application also up-regulated the expression of key antioxidant stress-responsive enzymes in *Gossypium hirsutum* (Venkatachalam et al. 2017b) and *Oryza sativa* (Salah et al. 2015). Contradictorily, exposure to nZnO in wheat enhanced generation of reactive oxygen species and adversely changed antioxidant defense systems and consequently led to destruction of the crucial cellular structure, especially membranes, and growth inhibition (Tripathi et al. 2017).

Conclusion

Due to the high consumption of nanoproducts, the entering likelihood of these nanoparticles into the food chain, especially through plant-derived foods/drugs, is inevitable. This study provides a valuable theoretical basis and insight into the potential advantage and toxicity of nSe and nZnO in pharmaceutically substantial plant lemon balm. Moreover, the comparative information about the nSe and nZnO with their bulk counterparts was also presented. Evidence was provided on eco-toxicological significance of nSe as a pollutant in plants. However, more convincing studies are required to illustrate the elusive eco-toxicological impacts of these nanoproducts. The nanoforms were more effective than their bulk counterparts to influence plant growth and physiology. Based on the findings, the simultaneous supplementation of nutrient solution with suitable doses of nSe and nZnO may improve plant growth, metabolism, and protection via critical mechanisms. These mechanisms are found to be improving nutritional status, modifying enzymatic and non-enzymatic antioxidant system, altering phytohormonal balances, influencing nitrogen assimilation, affecting gene expression pattern, inducing phenylpropanoid metabolism, and reinforcing root system. It should be mentioned that molecular evidence on the roles of trace nutrients, such as Se, is rare; the contributed mechanisms are elusive and require to be further explored. It is important to note that this experiment was conducted in the soilless condition to keep the concentrations almost constant. In case of using soil, the concentrations would not remain the same (it increases gradually) which could lead to more toxicity compared to the results of the present study. Moreover, the soil complexity and the existence of a multitude of factors, like pH, texture, organic contents, and microbiome make it

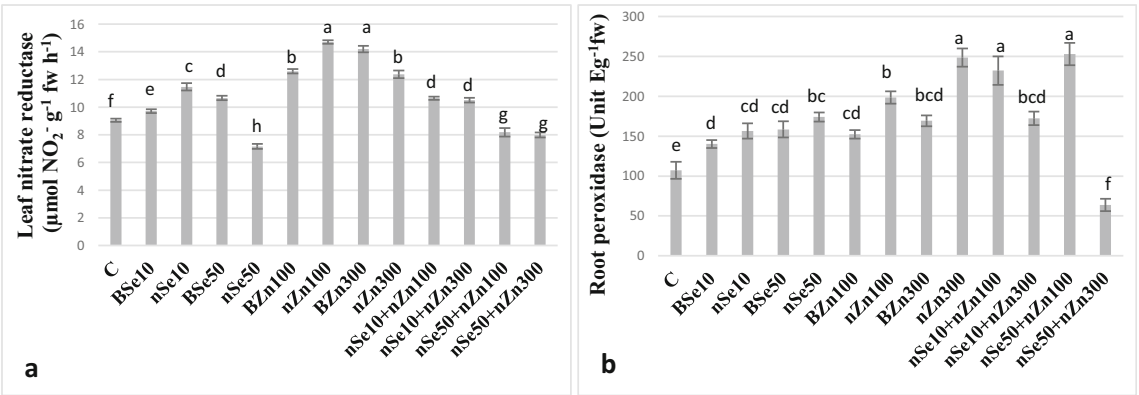

Fig. 9 **a**, **b** The induced alterations in activities of two key enzymes (nitrate reductase and peroxidase) in response to the manipulation of Hoagland nutrient solution with different concentrations of nSe, nZnO, and their bulk counterparts. Bars indicate the standard error

difficult to figure out the plant responses to nanoparticles in natural soil environments. These achievements can be employed to develop an alternative formulation for a nutrient solution and might be applied in food, agriculture, and related industries. This is the first evidence which focuses on both the beneficial and adverse roles of nZnO and nSe, especially in pharmaceutically substantial plants. Further studies on such formulations are required for future.

Acknowledgments The authors would like to thank Dr F. Gaziani (University of Tehran Science and Technology Park), Dr K. Khosraviani, Dr N. Oraghi Ardebili, and MSc Q. Asgari for their benevolent and professional collaborations in the research procedure.

Author's contribution All authors contributed to the conception and design of the study, drafting the articles, and revising it. All authors have contributed, seen, and approved the manuscript.

Compliance with ethical standards

Conflict of interest The authors declare that they have no conflict of interest.

References

Ardebili ZO, Ardebili NO, Jalili S, Safiallah S (2015) The modified qualities of basil plants by selenium and/or ascorbic acid. Turk J Bot 39(3):401–407

Asgari-Targhi G, Iranbakhsh A, Ardebili ZO (2018) Potential benefits and phytotoxicity of bulk and nano-chitosan on the growth, morphogenesis, physiology, and micropropagation of *Capsicum annuum*. Plant Physiol Biochem 127:393–402

Babajani A, Iranbakhsh A, Ardebili ZO, Eslami B (2019) Seed priming with non-thermal plasma modified plant reactions to selenium or zinc oxide nanoparticles: cold plasma as a novel emerging tool for plant science. Plasma Chem Plasma Process 39(1):21–34

Bouain N, Shahzad Z, Rouached A, Khan GA, Berthomieu P, Abdelly C, Poirier Y, Rouached H (2014) Phosphate and zinc transport and signalling in plants: toward a better understanding of their homeostasis interaction. J Exp Bot 65(20):5725–5741

Bradfield SJ, Kumar P, White JC, Ebbs SD (2017) Zinc, copper, or cerium accumulation from metal oxide nanoparticles or ions in sweet potato: yield effects and projected dietary intake from consumption. Plant Physiol Biochem 110:128–137

De Francisco EV, García-Estepa RM (2018) Nanotechnology in the agrofood industry. J Food Eng 238:1–11

De la Rosa G, López-Moreno ML, de Haro D, Botez CE, Peralta-Videa JR, Gardea-Torresdey JL (2013) Effects of ZnO nanoparticles in alfalfa, tomato, and cucumber at the germination stage: root development and X-ray absorption spectroscopy studies. Pure Appl Chem 85(12):2161–2174

Del Longo OT, González CA, Pastori GM, Trippi VS (1993) Antioxidant defences under hyperoxygenic and hyperosmotic conditions in leaves of two lines of maize with differential sensitivity to drought. Plant Cell Physiol 34(7):1023–1028

Djanaguiraman M, Belliraj N, Bossmann SH, Prasad PV (2018) High-temperature stress alleviation by selenium nanoparticle treatment in grain sorghum. ACS Omega 3(3):2479–2491

Domokos-Szabolcsy E, Marton L, Sztrik A, Babka B, Prokisch J, Fari M (2012) Accumulation of red elemental selenium nanoparticles and their biological effects in *Nicotinia tabacum*. Plant Growth Regul 68(3):525–531

Feng R, Wei C, Tu S (2013) The roles of selenium in protecting plants against abiotic stresses. Environ Exp Bot 87:58–68

Geneva M, Hristozkova M, Yonova P, Boychinova M, Stancheva I (2010) Effect of endomycorrhizal colonization with *Glomusin traradices* on growth and antioxidant capacity of *Sideritiss cardica* Griseb. Gen Appl Plant Physiol 36(1/2):47–54

Golubkina NA, Kosheleva OV, Krivenkov LV, Dobrutskaya HG, Nadezhkin S, Caruso G (2017) Intersexual differences in plant growth, yield, mineral composition and antioxidants of spinach (*Spinacia oleracea* L) as affected by selenium form. Sci Hortic 225:350–358

Hemeda HM, Klein BP (1990) Effects of naturally occurring antioxidants on peroxidase activity of vegetable extracts. J Food Sci 55(1):184–185

Hu T, Li H, Li J, Zhao G, Wu W, Liu L, Wang Q, Guo Y (2018) Absorption and bio-transformation of Selenium nanoparticles by wheat seedlings (*Triticum aestivum* L). Front Plant Sci 9

Iranbakhsh A, Ardebili ZO, Ardebili NO, Ghoranneviss M, Safari N (2018) Cold plasma relieved toxicity signs of nano zinc oxide in *Capsicum annuum* cayenne via modifying growth, differentiation, and physiology. Acta Physiol Plant 40(8):154

Javed R, Usman M, Yücesan B, Zia M, Gürel E (2017) Effect of zinc oxide (ZnO) nanoparticles on physiology and steviol glycosides production in micropropagated shoots of *Stevia rebaudiana*. Bertoni. Plant Physiol Biochem 110:94–99

Lee S, Kim S, Kim S, Lee I (2013) Assessment of phytotoxicity of ZnO NPs on a medicinal plant, Fagopyrum esculentum. Environ Sci Pollut Res 20(2):848–54

Lima LW, Pilon-Smits EA, Schiavon M (2018) Mechanisms of selenium hyperaccumulation in plants: **a** survey of molecular, biochemical and ecological cues. Biochim Biophys Acta (BBA)-General Subjects

Mehrian SK, De Lima R (2016) Nanoparticles cyto and genotoxicity in plants: mechanisms and abnormalities. Environ Nanotechnol Monitor Manage 6:184–193

Moghaddasi S, Fotovat A, Khoshgoftarmanesh AH, Karimzadeh F, Khazaei HR, Khorassani R (2017) Bioavailability of coated and uncoated ZnO nanoparticles to cucumber in soil with or without organic matter. Ecotoxicol Environ Saf 144:543–551

Moghanloo M, Iranbakhsh A, Ebadi M, Satari TN, Ardebili ZO (2019) Seed priming with cold plasma and supplementation of culture medium with silicon nanoparticle modified growth, physiology, and anatomy in *Astragalus fridae* as an endangered species. Acta Physiol Plant 41(4):54

Moradkhani H, Sargsyan E, Bibak H, Naseri B, Sadat-Hosseini M, Fayazi-Barjin A, Meftahizade H (2010) *Melissa officinalis* L, a valuable medicine plant: **a** review. J Med Plant Res 4(25):2753–2759

Mukherjee A, Sun Y, Morelius E, Tamez C, Bandyopadhyay S, Niu G, White JC, Peralta-Videa JR, Gardea-Torresdey JL (2016) Differential toxicity of bare and hybrid ZnO nanoparticles in green pea (*Pisum sativum* L): a life cycle study. Front Plant Sci 6:1242

Nazerieh H, Oraghi Ardebili Z, Iranbakhsh A (2018) Potential benefits and toxicity of nanoselenium and nitric oxide in peppermint. Acta Agric Slov 111(2):357–368

Rastogi A, Zivcak M, Sytar O, Kalaji HM, He X, Mbarki S, Brestic M (2017) Impact of metal and metal oxide nanoparticles on plant: a critical review. Front Chem 5:78

Safari M, Ardebili ZO, Iranbakhsh A (2018) Selenium nano-particle induced alterations in expression patterns of heat shock factor A4A (HSFA4A), and high molecular weight glutenin subunit 1Bx (Glu-1Bx) and enhanced nitrate reductase activity in wheat (*Triticum aestivum* L). Acta Physiol Plant 40(6):117

Salah SM, Yajing G, Dongdong C, Jie L, Aamir N, Qijuan H, Weimin H, Mingyu N, Jin H (2015) Seed priming with polyethylene glycol

regulating the physiological and molecular mechanism in rice (*Oryza sativa* L) under nano-ZnO stress. Sci Rep 5:14278

Seddighinia FS, Iranbakhsh A, Ardebili ZO, Satari TN, Soleimanpour S (2019) Seed Priming with Cold Plasma and Multi-walled Carbon Nanotubes Modified Growth, Tissue Differentiation, Anatomy, and Yield in Bitter Melon (*Momordica charantia*). J Plant Growth Regul. https://doi.org/10.1007/s00344-019-09965-2

Sheteiwy MS, Dong Q, An J, Song W, Guan Y, He F, Huang Y, Hu J (2017) Regulation of ZnO nanoparticles-induced physiological and molecular changes by seed priming with humic acid in *Oryza sativa* seedlings. Plant Growth Regul 83(1):27–41

Subbaiah LV, PrasadTNVKV KTG, Sudhakar P, Reddy BR, Pradeep T (2016) Novel effects of nanoparticulate delivery of zinc on growth, productivity, and zinc biofortification in maize (*Zea mays* L). J Agric Food Chem 64(19):3778–3788

Tamaoki M, Freeman JL, Marques L, Pilon-Smits EAH (2008) New insights into the roles of ethylene and jasmonic acid in the acquisition of selenium resistance in plants. Plant Signal Behav 3(10):865–867

Tang W, Dang F, Evans D, Zhong H, Xiao L (2017) Understanding reduced inorganic mercury accumulation in rice following selenium application: selenium application routes, speciation and doses. Chemosphere 169:369–376

Tonelli M, Pellegrini E, D'Angiolillo F, Petersen M, Nali C, Pistelli L, Lorenzini G (2015) Ozone-elicited secondary metabolites in shoot cultures of *Melissa officinalis* L. Plant Cell Tissue Organ Cult 120(2):617–629

Tripathi DK, Mishra RK, Singh S, Singh S, Singh VP, Singh PK, Chauhan DK, Prasad SM, Dubey NK, Pandey AC (2017) Nitric oxide ameliorates zinc oxide nanoparticles phytotoxicity in wheat seedlings: implication of the ascorbate-glutathione cycle. Front Plant Sci 8:1

Venkatachalam P, Jayaraj M, Manikandan R, Geetha N, Rene ER, Sharma NC, Sahi SV (2017a) Zinc oxide nanoparticles (ZnONPs) alleviate heavy metal-induced toxicity in *Leucaena leucocephala* seedlings: a physiochemical analysis. Plant Physiol Biochem 110:59–69

Venkatachalam P, Priyanka N, Manikandan K, Ganeshbabu I, Indiraarulselvi P, Geetha N, Muralikrishna K, Bhattacharya RC, Tiwari M, Sharma N, Sahi SV (2017b) Enhanced plant growth promoting role of phycomolecules coated zinc oxide nanoparticles with P supplementation in cotton (*Gossypium hirsutum* L). Plant Physiol Biochem 110:118–127

Wang X, Yang X, Chen S, Li Q, Wang W, Hou C, Gao X, Wang L, Wang S (2016) Zinc oxide nanoparticles affect biomass accumulation and photosynthesis in *Arabidopsis*. Front Plant Sci 6:1243

Weitzel C, Petersen M (2011) Cloning and characterisation of rosmarinic acid synthase from Melissa officinalis L. Phytochemistry 72(7):572–578

Wu Z, Liu S, Zhao J, Wang F, Du Y, Zou S, Li H, Wen D, Huang Y (2017) Comparative responses to silicon and selenium in relation to antioxidant enzyme system and the glutathione-ascorbate cycle in flowering Chinese cabbage (*Brassica campestris* L sspchinensisvarutilis) under cadmium stress. Environ Exp Bot 133:1–11

Xun H, Ma X, Chen J, Yang Z, Liu B, Gao X, Li G, Yu J, Wang L, Pang J (2017) Zinc oxide nanoparticle exposure triggers different gene expression patterns in maize shoots and roots. Environ Pollut 229:479–488

Zafar H, Ali A, Ali JS, Haq IU, Zia M (2016) Effect of ZnO nanoparticles on *Brassica nigra* seedlings and stem explants: growth dynamics and antioxidative response. Front Plant Sci 7:535

Zhu Z, Chen Y, Shi G, Zhang X (2017) Selenium delays tomato fruit ripening by inhibiting ethylene biosynthesis and enhancing the antioxidant defense system. Food Chem 219:179–184